Radiation-Induced Cross-Linking in a Silica-Filled Silicone Elastomer As Investigated by Multiple Quantum ^{1}H NMR

Robert S. Maxwell,*,† Sarah C. Chinn,† David Solyom,‡ and Rebecca Cohenour‡

Lawrence Livermore National Laboratory, 7000 East Ave, Livermore, California 94551, and Honeywell Inc. Federal Manufacturing & Technologies, Kansas City, Missouri 64141

Received November 17, 2004; Revised Manuscript Received May 24, 2005

ABSTRACT: DC745 is a commercially available silicone elastomer consisting of dimethyl, methyl−phenyl, and vinyl−methyl siloxane monomers cross-linked with a peroxide vinyl specific curing agent. It is generally considered to age gracefully and to be resistant to chemical and thermally harsh environments. However, little data exist on the radiation resistance of this commonly used silicone elastomer. We report static ^{1}H NMR studies of residual dipolar couplings in DC745 solid elastomers subject to exposure to ionizing γ radiation. ^{1}H spin-echo NMR data shows that with increasing dose the segmental dynamics decrease is consistent with radiatively induced cross-linking. ^{1}H multiple quantum NMR was used to assess changes in the network structure and observed the presence of a bimodal distribution of residual dipolar couplings, $\langle\Omega_d\rangle$, that were dose dependent. The domain with the lower $\langle\Omega_d\rangle$ has been assigned to the polymer network while the domain with the higher $\langle\Omega_d\rangle$ has been assigned to polymer chains interacting with the inorganic filler surfaces. In samples exposed to radiation, the residual dipolar couplings in both reservoirs were observed to increase, and the populations were observed to be dose dependent. The NMR results are compared to differential scanning calorimetry (DSC) and a two-step solvent swelling technique. The solvent swelling data lend support to the interpretation of the NMR results, and the DSC data show both a decrease in the melt temperature and the heat of fusion with cumulative dose, consistent with radiative cross-linking. In addition, DSC thermograms obtained following a 3 h isothermal soak at −40 °C showed the presence of a second melt feature at $T_m \sim -70$ °C consistent with a network domain with significantly reduced segmental motion.

Introduction

As polymeric materials are required to endure ever-increasing lifetimes in service, there is a fundamental need to employ sensitive and versatile in situ methods to investigate the structural and motional changes that occur in these materials as a result of use in chemically, thermally, or radioactively harsh environments. Ideally, these methods would allow a complete assessment of aging mechanisms in order to yield predictive capabilities. For example, it has been well recognized that time-dependent changes in network structure (e.g., domain sizes, morphology, and cross-link density) can contribute to degradation in engineering performance over decades, and numerous methods have been developed to assess such changes. It is, in addition, generally understood that changes in the physical and chemical interactions between reinforcing fillers and the polymer network will also contribute to the long-term performance of filled elastomeric components. There are few spectroscopic techniques, however, that are generally capable of probing this regime.

Nuclear magnetic resonance (NMR) has gained much attention in the past few decades for its ability to nondestructively characterize changes in chemical composition and network structure in a broad range of polymer systems.[1−25] Static ^{1}H multiple quantum NMR methods which measure the residual dipolar couplings, in specific, hold much promise for such efforts.[13−20,24] In elastomeric materials, the residual dipolar couplings have been shown to be the result of topological constraints interfering with fast reorientations on the NMR time scale that otherwise would be expected to average homonuclear dipolar couplings to zero.[9] The residual dipolar couplings, in fact, have been shown to be quite sensitive to network and morphological changes and have been used to test theories of polymer structure, ordering, and dynamics. These residual dipolar couplings can be quantitatively assessed using a variety of NMR experimental protocols, including relaxation methods, ^{2}H and ^{1}H line-shape analysis, modulation of the stimulated echo, and the magic echo which has been shown to be superior for assessing residual dipolar couplings than either the solid echo or the stimulated echo.[4−25]

More recently, it has been reported that the characterization of the growth of multiple quantum coherences can provide detailed insight into silicone network structure by increasing the selectivity of the NMR experiment to the structure and dynamics most connected to the topology of the polymer network, including chain ordering at the surface of inorganic filler particles.[13−24] In addition, it has been shown that echo-based methods can overestimate the residual dipolar couplings due to the effects of magnetic susceptibilities and field gradients due to internal microscopic voids and the inorganic filler.[28] These effects have been observed to be large enough to reverse trends of $\langle\Omega_d\rangle$ vs cross-link density at different fields.[29,30] MQ based approaches, have so far, been shown to be insensitive to these effects.[30] Since the network topology and the filler−particle interactions determine to a significant part the engineering properties,[31] including tensile, shear, and creep moduli, MQ methods offer the potential for model free insight into the origins of degradation in material performance.

* Corresponding author: Tel (925) 423-4991, (925) 422-3750, e-mail maxwell7@llnl.gov.
† Lawrence Livermore National Laboratory.
‡ Honeywell Inc. Federal Manufacturing & Technologies.

10.1021/ma047625s CCC: $30.25
Published on Web 07/15/2005

In this paper, we examine the effects of radiation dose on the microstructure and polymer chain mobility of DC-745, a complex, commercial, cross-linked, and filled silicone elastomer using static ^{1}H echo and multiple quantum NMR methods. These methods provide insight into the changes in both the network structure and the polymer−filler interface. The data are interpreted in combination with solvent swelling and DSC studies. Though there has been significant application of NMR to silicone-based polymeric materials (see, for example, refs 4−9,17−19, 22, and 23), no systematic study of the effects of radiation on DC745 nor the application of these multiple quantum methods to radiation-induced damage at the filler−polymer interface in silicones has been reported previously.

Experimental Section

Samples were cured from Dow Corning 745U silicone fluid with 2,5-dimethyl-2,5-di(*tert*-butylperoxy)hexane peroxide curing agent supported on $CaCO_3$ (Dow Corning). DC745U fluid is a proprietary mixture of monomer composition. ^{1}H and ^{29}Si{^{1}H} NMR have determined that the elastomers studied here contained ∼98.5% dimethylsiloxane monomers, ∼1.5% methylphenylsiloxane monomers, and a small amount of vinylsiloxane monomers that are converted to short chain (presumably $N = 4$) alkyl cross-linking junctions. Curing was performed by thermal activation at 170 °C for 10 min. The final elastomer also contains ∼30 wt % mixture of quartz and high surface area fumed silica fillers and small amounts of $CaCO_3$ remaining from the curing agent for thixotropic thickening and tear resistance. The fully cured composites were sealed in glass ampules evacuated and backfilled with N_2. The ampules were then placed in a 1 L stainless steel canister and lowered into the irradiation pit. The irradiation pit contained a Co-60 source (1.2 MeV). The samples were irradiated at 5 kGy/h for times necessary to expose the samples to 30−250 kGy.

DSC analyses were performed (TA Instruments, MDSC Q1000, New Castle, DE) by cooling the sample at a rate of 1.50 °C/min to −160 °C from room temperature. Subsequent heating of the samples was then performed at 1.50 °C/min with a modulation frequency of ±0.16 °C/40 s. The pristine copolymer was characterized by a crystallization temperature at −45 °C and a glass transition temperature at −120 °C. A second set of analyses were then performed that included a 3 h isothermal soak at −80 °C on the cool down cycle.

Details of the two-step solvent swelling based on the method developed by Polmanteer and Lentz have been described elsewhere.[6−8,32−34] The samples (∼1 g) were first weighed for the initial dry weight and then submerged in 600 mL of toluene (Aldrich, Milwaukee, WI) in a sealed Teflon container while stirring. Periodically, the swollen weight of the sample was measured until an equilibrium weight was obtained (∼ 3 days). Once saturation equilibrium had been established, 150 mL of concentrated ammonia (28 wt %, Aldrich, Milwaukee, WI) was added directly to the toluene solution, the container was resealed, and stirring continued. The ammonia effectively severs the hydrogen-bonding interaction between the surface silanols on the filler and the siloxane backbone of the polymer. The ammonia is of limited solubility in toluene, and it is expected that only a fraction of the ammonia enters the polymer−toluene phase and that the toluene−ammonia mixture is likely still a good solvent for the siloxane polymers studied here. Each sample was again weighed periodically until equilibrium was reached with the toluene/ammonia mixture (∼30 days). The samples were then dried overnight under vacuum or under ambient conditions for 7 days and reweighed for the final dry weight. The weights were then used in a modified Flory−Higgins approach discussed in detail in ref 6 to obtain the cross-link densities due to the polymer network, ν_{poly}, the polymer and the filler, ν_{filler}, and the total cross-link density, ν_{total}, where $\nu_i = MW_{monomer}/MW_{i-cross-links}$ and $MW_{i-cross-links}$ is the molecular weight between cross-links derived from the Flory−Higgins equation. As mentioned in refs 6 and 7, the molecular weights between cross-links are additive (i.e., $MW_{polyl} = MW_{total} + MW_{filler}$) and not the cross-link densities. All the volume fractions calculated were corrected for the volume of the filler, which would not swell. Given the unknown nature of the polymer formulation, including the exact filler content, the cross-link densities should be considered measures of cross-link density relative to each other and not absolute.

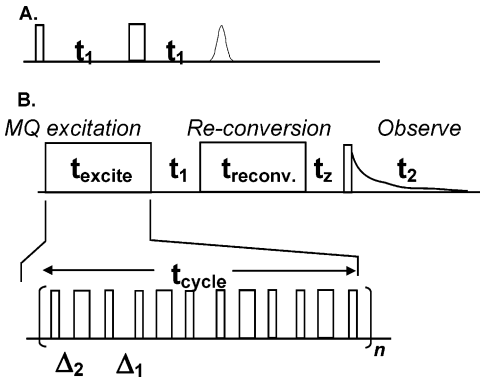

Figure 1. Pulse sequences used in this study: (A) Hahn echo; (B) multiple quantum excitation, reconversion, and observe sequence. Details of pulse phases and delays are discussed in the text.

All ^{1}H NMR measurements were performed at 400.13 MHz on a Bruker Avance 400 spectrometer using a Bruker TBI (HCX) 5 mm probe. ^{1}H $\pi/2$ excitation pulses of 6 μs and relaxation delays of 7 s were used. In all cases, small (0.1 cm × 0.1 cm × 0.1 cm) squares of elastomer were cut from a larger piece and set in the portion of a 5 mm NMR tube that would be within the coil volume of the probe. Spin-echo decay curves were obtained using a standard Hahn-echo sequence shown in Figure 1A with delays between pulses ranging from 10 μs to 40 ms. The echo decay curves were normalized to the extrapolated $t = 0$ intensity. These normalized curves were then fit to a biexponential decay, including a term for non-exponential decay due to residual dipolar couplings:[9]

$$EI(t) = X_A \exp(-2t/T_{2b} - \langle\Omega_d^2\rangle\tau_s^2 \exp(t/\tau_s) + t/\tau_s - 1) + X_B \exp(-2t/T_{2b}) \quad (1)$$

where the A terms represent the monomers associated with the cross-linked network structure (with a mean square of the residual dipolar couplings of $\langle\Omega_d^2\rangle$ and motional correlation time τ_s), while the B terms represent the monomers associated with the nonnetwork sol fraction and dangling chain ends characterized by a negligible residual dipolar coupling. It should be noted that due to the number of competing contributions to the echo decay rate, $\langle\Omega_d^2\rangle$ can usually only be diagnostic of trends in cross-link density or molecular order, and even these trends must be interpreted with care given previous observations that the trends can be field dependent.[29,30]

Multiple quantum NMR experiments were performed using the refocused multiple quantum excitation and reconversion pulse sequence shown in Figure 1B. This sequence was shown to be a versatile method for exciting MQ coherences in silicone systems.[17,18] The phases of the reconversion sequence were cycled in 90° steps with phase inversion on the observe pulse for coherence selections. (The pulse sequence excited all even multiple quantum coherences.) CYCLOPS was then added to yield a 16-step phase cycle.[17,18] As described in ref 17, the pulse sequence yields the total sum of the even multiple quantum coherences, significantly dominated by the double quantum coherences, S_{mq} ($S_{2Q} > 5S_{4Q}$). Pulse lengths of 6 μs were used with delay Δ_1 and Δ_2 equal to 4.83 μs and 6.16 μs, respectively, leading to a cycle time, τ_c, of 182 μs and scaling factor, a, of 0.611. Repeat experiments with increased values of Δ_1 and Δ_2

showed no discernible differences, indicating that at the delays used no significant distortions due to high duty cycles were observed.[17] The effective evolution time is then given by $t_e = at_c$.

This set of data was then normalized with the use of a reference data set, S_{ref}, obtained by removing the alternating phases on the observe pulse. The reference is the sum of all coherences that have not evolved into even quantum coherences.[17] The reference signal was first modified by subtracting the long time decay component assigned to the sol fraction of the polymer network, $S^*_{ref}(t_e) = S_{ref}(t_e) - S_{ref-long}(t_e)$.[17] The normalized multiple quantum integral was obtained by calculating for each effective excitation time, t_e

$$I_{mq}(t_e) = S_{mq}(t_e)/(S_{mq}(t_e) + S^*_{ref}(t_e)) \quad (2)$$

The referencing of the MQ data set by the reference data set serves to remove the long-term decays caused by slow dynamics and transverse relaxation processes and provides a more convenient data set to analyze. This method can be subject to systematic errors in the deconvolution state, as discussed below. Alternate normalization methods have been described in the literature, most notably as determined from a density matrix formulism, simply by the intensity after a $\pi/2$ excitation pulse.[13] Normalization using the signal intensity after a single pulse, however, requires a more complex fitting scheme in which the long-term decay must also be considered in addition to the initial short term growth. The method described by Schneider et al. requires approximately half the acquisition time for a complete data set.[13]

For the normalization method used here, semiempirical mathematical descriptions of the MQ growth have been developed by Saalwächter.[17] In the case of spins characterized by a dominant residual dipolar coupling, and where the double quantum intensity dominates the higher order terms, the multiple quantum growth curve can then described by

$$I_{mq}(t_e) = A(1 - \exp(-B(\langle\Omega_d\rangle/2\pi)^2 t_e^{\,2}) \quad (3)$$

In cases where spins can be described by more than one residual dipolar couplings, as in the case of phase-separated network structures with discrete and well-separated mean residual dipolar couplings, the multiple quantum growth curves can be described by a summation of growth curves

$$I_{mq}(t_e) = \Sigma X_i(1 - \exp(-B(\langle\Omega_d\rangle_i/2\pi)^2) t_e^{\,2}) \quad (4)$$

where X_i is the mole fraction of spins that can be described by $\langle\Omega_d\rangle_i$. Such multidomain contribution MQ growth curves have been observed in silicone polymers[17] and in thin layers of PDMS spin-coated on silica substrates.[19,25] The MQ NMR data obtained and analyzed in this report were fit to eqs 3 and 4 using a least-squares multivariable fit (X_1, $\langle\Omega_d\rangle_1$, and $\langle\Omega_d\rangle_2$) in Matlab. The fits were performed only up to $I_{mq}(t_e) = 0.45$. The method presented here has been shown to be subject to systematic errors.[17] These include an overestimation of the more strongly coupled spins, an insensitivity to small quantities of spins with very low $\langle\Omega_d\rangle$, and a underestimation of the absolute couplings by less than 5%—due to neglect of longer range couplings.

The theory governing the effects of anisotropic motion on the dipolar couplings between proton nuclear spins is well established.[9,14,17,35] The dipolar couplings between spins i and j in the absence of motion, $\langle\Omega_d\rangle^{(i,j)}_{static}$, is generally given by the following equation:[31]

$$\langle\Omega_d\rangle^{(i,j)}_{static} = \mu_0\gamma_H{}^2 h/8\pi r_{ij}^{\,3} \quad (5)$$

where μ_0 and γ_H are the permitivtiy of free space and the gyromagnetic ratio for protons and r_{ij} is the internuclear distance. It has been shown the for PDMS polymers $\langle\Omega_d\rangle_{static}$ is 8.9 kHz.[36] In the case of fast chain motions restricted by topological constraints typical in polymeric melts, the dipolar coupling is attenuated to[9,14,17]

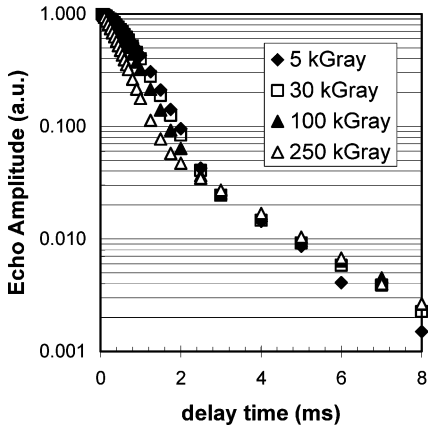

Figure 2. Hahn-echo decay curves for irradiated elastomers for cumulative doses of 5, 30, 100, and 250 kGy.

$$\langle\Omega_d\rangle^{(i,j)}_{motion} = \langle\Omega_d\rangle^{(i,j)}_{static} S_b \cdot {}^1/_2\langle 3\cos^2\alpha - 1\rangle \quad (6)$$

where α is the angle between the internuclear vector and the polymeric chain segment orientation—averaged over all the fast motions—and S_b is the dynamic order parameter. In the following $\langle\Omega_d\rangle^{(i,j)}_{motion}$ will take the designation $\langle\Omega_d\rangle$. In the case of simple Gaussian chain statistics, it has been shown that

$$S_b = {}^3/_5 r^2/N \quad (7)$$

where N is the number of segments between topological constraints and $r = \mathbf{R}/\mathbf{R}_0$, the deviation of the chain end-to-end vector $\mathbf{R}$ from its average value, $\mathbf{R}_0$. Substituting for $\langle\Omega_d{}^2\rangle$ and the average cross-link density υ_{total} leads to the general proportionality

$$\langle\Omega_d{}^2\rangle = N^{-2} = \upsilon_{total}{}^2 \quad (8)$$

Invoking standard assumptions in polymer network theory, it has been shown that the residual dipole coupling is also proportional to square of the shear modulus, G'.[7]

Results and Discussion

Hahn-echo decay curves for the irradiated DC745 samples are shown in Figure 2 and are characterized by (a) bimodal decay, (b) nonexponential decay behavior, and (c) dose-dependent change in decay rate. The bimodal decay is a common observance in ^{1}H NMR relaxation studies of silicone polymers.[4−9] Following these studies, the rapidly decaying component is assigned to the proton spins in the cross-linked network while the slower decaying component is assigned to the nonnetwork, sol species. The nonexponential decay rate has also been observed previously in silicone elastomers and is a consequence of the anisotropic motions, causing incomplete averaging of the dipolar couplings leading to mixed Gaussian (solidlike) and exponential (liquidlike) decay.[9]

The decay curves in Figure 2 have been fit to eq 1, and the dose-dependent mean-squared residual dipolar couplings, $\langle\Omega_d{}^2\rangle$, are shown in Figure 3 and listed in Table 1 and indicate a steady, but nonlinear, increase in $\langle\Omega_d{}^2\rangle$ with dose. Extracted residual dipolar couplings have been shown to be closely related to the segmental dynamics, the average cross-link density, and the elastic modulus in a broad range of silicone elastomer systems as discussed in eqs 5−8. Though such methods can be used to track relative changes in these parameters, early

Table 1. Results of Experimental Parameters for Samples Studied[a]

dose (kGy)	$\nu_{polymer}$ {$\times 10^4$}	ν_{total} {$\times 10^4$}	ν_{filler} {$\times 10^4$}	X_{long} (± 2)	$\langle\Omega_d^2\rangle$ ($\times 10^5$ rad^2 s^{-2})	X_1	$\langle\Omega_d\rangle_1$ (rad/s)	$\langle\Omega_d\rangle_2$ (rad/s)
5	4.98	10.49	9.50	9.5	2.1	0.89	700	3200
10	5.27	10.74	10.35	11.5	2.1	0.87	702	3000
30	6.25	11.77	13.33	10.2	2.3	0.86	717	3095
50	5.98	13.25	10.90	10.2	2.6	0.85	803	3376
100	7.52	15.62	14.50	10.0	3.1	0.81	806	3190
250	11.25	24.12	21.09	11.0	6.0	0.75	1113	3900

[a] ν_i values from solvent swelling experiments; X_{long} and $\langle\Omega_d^2\rangle$ from Hahn-echo experiments; X_1, $\langle\Omega_d\rangle_1$, and $\langle\Omega_d\rangle_2$ from MQ experiments.

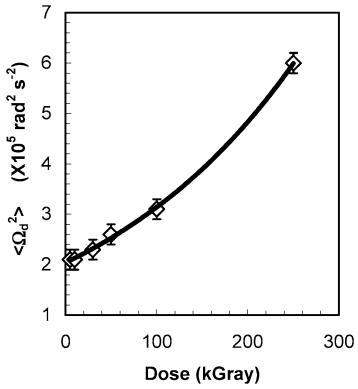

Figure 3. Mean-square residual dipolar coupling, $\langle\Omega_d^2\rangle$, of irradiated elastomers from solid-echo decay curves as a function of cumulative dose.

studies have shown that these methods tend to overestimate the residual dipolar couplings and thus the dynamic order parameters due to contributions from motions and couplings over a large range of time and length scales and the influence of diffusion of spins through field gradients resulting from internal microscopic voids and/or the inorganic filler surface.[28] The results of such measurements yield potentially misleading conclusions on network ordering. In addition, in the experiments performed here, no spectroscopic signature or relaxation time was observed which could be correlated to the polymer chains directly interacting with the filler surface.

Multiple quantum methods, on the other hand, have shown to be much more selective to network dynamics in the millisecond time scale and are dominated by the residual dipolar couplings between spins within the six methyl groups in each monomer. As a result, MQ-NMR has been shown to be more selective to local network structure and dynamics.[13−20] Typical curves for the various network models are shown in Figure 4. A network behaving as a single network with a single residual dipolar coupling is shown in Figure 4A and described by eq 3. This is the case that would be expected for a monomodal network. Three curves are shown with increasing residual dipolar coupling and show that as the segmental dynamics decrease, raising the residual dipolar coupling, the rate of MQ coherence growth increases. For the case of phase-separated domains with well-separated network structures, as in the case of network polymer chains and polymer chains strongly interacting with the inorganic filler surface, the multiple quantum growth curve reveals itself as a dual growth curve with dual inflection points, as shown in Figure 4B. In the case of a broad distribution of residual dipolar couplings, due for example to a distribution of chain lengths that would be expected in a random crosslinked polymer, the growth curve is predicted, as shown in ref 17, to produce a MQ growth curve shown in Figure 4C with a slow long time growth term.

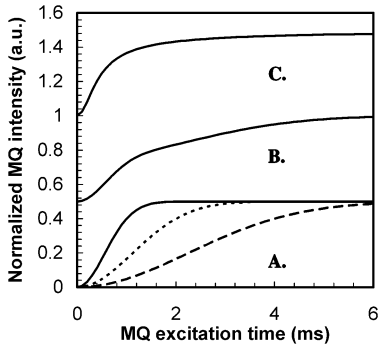

Figure 4. Representative plot of I_{MQ} as a function of MQ mixing time for (A) increasing values of the residual dipolar coupling, $\langle\Omega_d\rangle = 400$, 600, and 800 rad/s; (B) dual morphology model, described by eq 8 with equal populations of sites with $\langle\Omega_d\rangle_1 = 400$ and $\langle\Omega_d\rangle_2 = 1000$ rad/s; (C) distribution of residual dipolar couplings, described in ref 17 centered at 600 rad/s with a Gaussian width of 100 rad/s. (B) and (C) have been vertically offset for clarity.

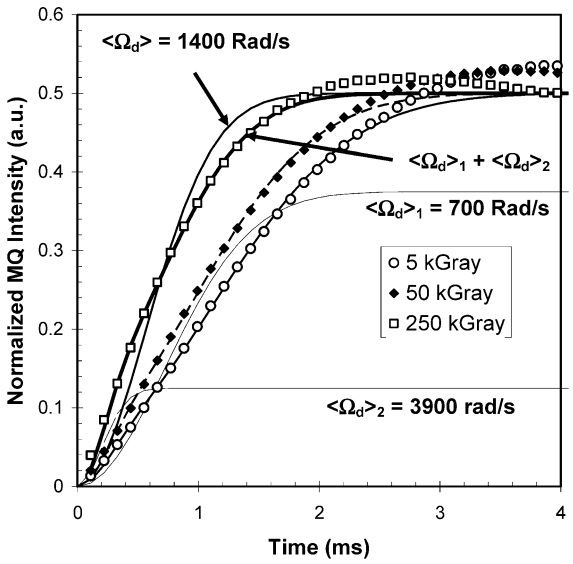

Figure 5. Experimental MQ growth curves, I_{MQ}, vs mixing time for irradiated elastomers with cumulative doses of 5, 50, and 250 kGy. Lines are simulated growth curves assuming either single or dual residual dipolar couplings: (A) single $\langle\Omega_d\rangle$ with $X_1 = 0.25$; (B) single $\langle\Omega_d\rangle$ with $X_2 = 0.75$; (C) sum of (A) and (B); (D) best fit of 250 kGy growth curve to a single $\langle\Omega_d\rangle$.

Multiple quantum growth curves for the 5, 50, and 250 kGy radiatively aged samples are shown in Figure 5. The initial growth rate was clearly observed to be dose dependent with higher exposures leading to higher growth rates. Fits of the data using eq 3 were only acceptable for the low dose exposures. As the dose increased, it became increasingly difficult to fit the growth curves with only one site. As a result, we choose to consider two possibilities for fitting the MQ growth curves: (a) a distribution of residual dipolar couplings and (b) a bimodal distribution of dipolar couplings. As

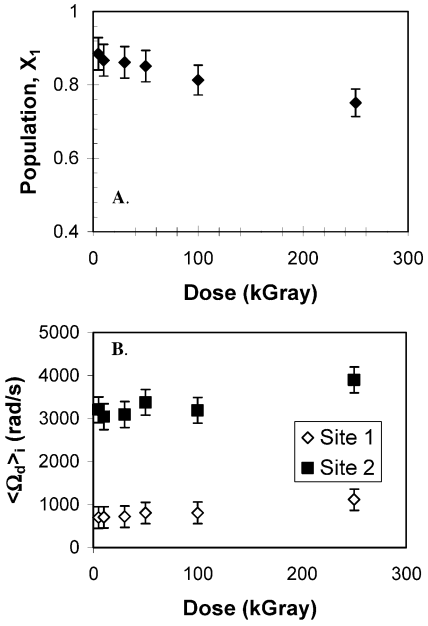

Figure 6. Results of three parameter fits to eq 8 of $I_{MQ}(t)$ curves shown in Figure 7 as a function of cumulative dose: (A) changes in mole fraction, X_1; (B) changes in residual dipolar couplings, $\langle\Omega_d\rangle_1$ and $\langle\Omega_d\rangle_2$.

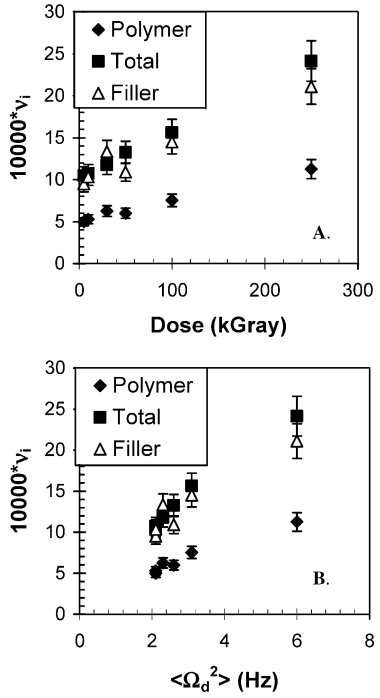

Figure 7. (A) Cross-link densities, ν_{poly}, ν_{total}, and ν_{filler}, of irradiated elastomers obtained from two-phase solvent swelling experiments as a function of cumulative dose. (B) Plot of ν_{poly}, ν_{total}, and ν_{filler} as a function of mean-square residual dipolar coupling from spin-echo studies, $\langle\Omega_d^2\rangle$, for irradiated elastomers.

can be seen in Figure 4, a broad distribution of residual dipolar couplings leads to a long excitation term in the 5−10 ms range. This was not observed in the materials studied here. This suggests a narrow distribution of couplings is present. The observations of narrow distributions was also observed in the bimodal networks studied by Saalwätcher.[17] A fit of the MQ growth curves to a bimodal superposition of a relatively large coupling and a lower coupling using eq 4, however, did adequately reproduce the experimental data, as can be seen in Figure 5. This indicates that there are two distinct network domains in this material. The domain with lower residual dipolar couplings is likely due to the general network polymer chains. The chains associated with the higher residual dipolar couplings we assign to polymer chains either physically or chemically interacting with the silica filler surface or in a domain with significantly higher cross-link density than the more dominant network chains. It has been shown by both NMR and dielectric relaxation studies that surface adsorbed polymers are generally characterized by a reduction in the segmental dynamics.[11,19,37−40] Given the lack of any further information regarding the network structure in these composites and the solvent swelling and DSC data below, it is likely that the high residual dipolar coupling spins reside in chains associated with the silica surface.

Results of the fit to eq 4 for a bimodal distribution of residual dipolar couplings are shown in Figure 6 and are listed in Table 1. At low doses, the NMR results suggest the network is dominated (∼89% of monomers) by low residual dipolar couplings near 700 rad/s. The remaining network monomers are in a domain with significantly higher residual dipolar coupling near 3200 rad/s. As the dose increased, the residual dipolar couplings in each domain increased from ∼700 to ∼1100 rad/s and from ∼3200 to ∼3900 rad/s while the mol % in each domain also changed, with the more ordered network equilibrating with the less ordered network (5 kGy, $X_{high} = 0.11$, $X_{low} = 0.89$; 250 kGy, $X_{high} = 0.25$, $X_{low} = 0.75$). Assuming a 30 wt % filler content with a surface area of ∼300 m^2/g, of which 25% are accessible to the polymer, and four monolayers with a thickness of ∼0.7 nm each,[24] it is estimated that the adsorbed chains would make up ∼10 wt %. Previous studies using both ^{29}Si $\{^1H\}$ cross-polarization methods and solvent swelling methods (see below) have shown that high doses of radiation can cause covalent bonding of the polymer chains to the inorganic surface.[6,7,41,42] The data obtained here are consistent with a scenario in which radiation causes not only random cross-linking in the polymer network but also the increasingly thick layer of polymeric chains interacting either directly or indirectly with the inorganic surface.

The NMR studies reported below were then validated with solvent swelling studies and thermal methods. Calculated cross-link densities from equilibrium swelling weights are shown in Figure 7 and show that with increasing dose the cross-link density increased not only in the overall cross-link density, υ_{total}, but also in the both the contributions due to the polymer network, υ_{poly}, and the filler−polymer interaction, υ_{filler}. In general, the solvent swelling data show that with exposure to γ-radiation in an N_2 atmosphere radiative cross-linking occurred in the polymer network. The increase in the contribution due to the filler−polymer interaction, in particular, indicates that the number of polymer chains influenced by hydrogen bonding to the filler surface increased with exposure to radiation, consistent with our assignment of the high residual coupling chains to surface adsorbed chains. Comparisons of the residual dipolar couplings obtained from the spin-echo and MQ studies with the cross-link densities determined from solvent swelling are shown in Figure 8 and show reasonable agreement with the trends predicted by eq 8.

DSC thermograms with and without a 3 h isothermal soak at −40 °C of the radiativley aged materials are

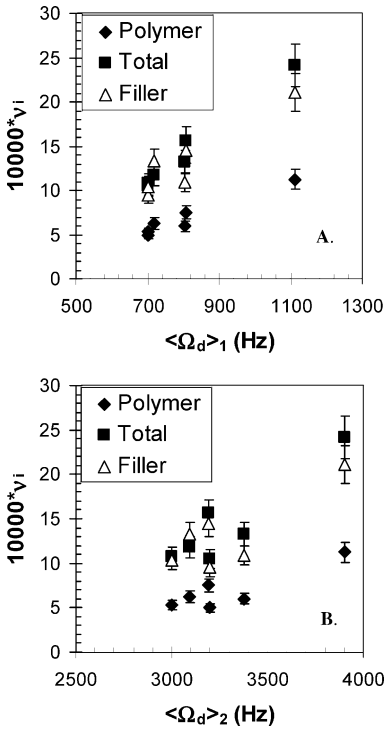

Figure 8. Plot of cross-link density as a function of residual dipolar couplings from MQ-NMR experiments. Cross-link densities derived from two-phase solvent swelling experiments: (A) ν_{poly}, ν_{total}, and ν_{filler} vs $\langle\Omega_d\rangle_1$; (B) ν_{poly}, ν_{total}, and ν_{filler} vs $\langle\Omega_d\rangle_2$.

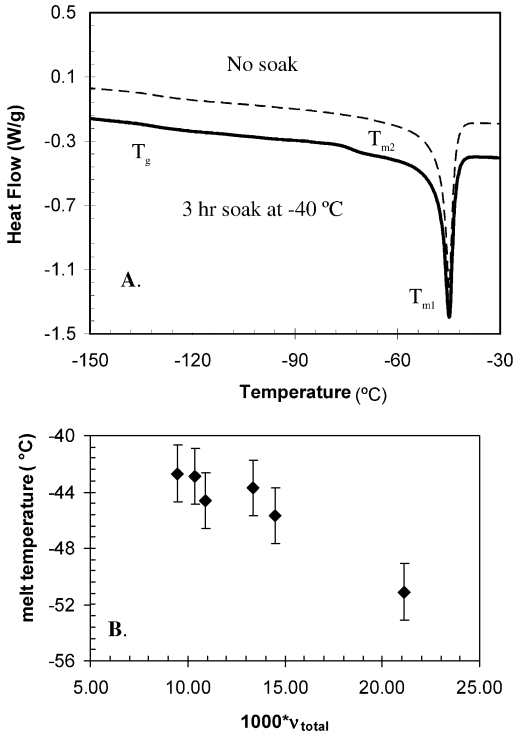

Figure 9. (A) Melting portion of DSC thermograms for elastomers irradiated to the indicated cumulative dose. Dashed line: no isothermal soak; solid line: obtained with isothermal soak of 3 h at −80 °C. Curves clearly indicate dose-dependent changes in melt temperature and melt heat of fusion. (B) Change in melt temperature, T_m, as a function of cumulative dose for irradiated samples.

shown in Figure 9. The thermograms obtained without a isothermal soak were characterized by a glass transition temperature, T_g, at ∼−120 °C and a melting endotherm in the heating curve at $T_m = -40$ °C. T_g was not observed to be a function of cumulative dose in these samples while both T_m and the heat of fusion, ΔH_m, were observed to decrease with cumulative dose and increased cross-link density. This observation is consistent with the increased cross-link density seen in the NMR and solvent swelling data. We have previously reported that for a different filled PDMS/PDPS formulation the heat of melting depended on cumulative dose exposure to γ-radiation.[8] With increasing dose, the heat of melting steadily decreased because for a given dwell time at low temperatures a decreasing fraction of chains were able to rearrange for crystallization. As can be seen in Figure 9B, the heat of melting for the irradiated materials steadily decreases with increasing dose. As shown in refs 6 and 8, a portion of this decrease could be recovered if the dwell time at low temperature was increased due to dramatic changes in the crystallization kinetics.[8] Thermograms of samples subject to a 3 h isothermal soak at −80 °C are shown in the lower curve of Figure 9A. No appreciable change in ΔH_m was noted for any of the samples, indicating that for the dominant melt peak the kinetics of crystallization are rapid. A new broad melt feature, however, centered at about $T_{m2} = -72$ °C was observed in all samples subject to the isothermal soak. This feature likely represents melting of network chains subject to fewer degrees of motional freedom, i.e., sites near locally higher cross-link density or sorbed at the filler interface. In siloxane polymers, a change in T_m of 20 °C would require a difference in cross-link density of ∼400%.[8] Deconvolution of the DSC thermogram suggests that these chains may represent as much as 5−10% of the polymer chains melting. Though DSC is not generally considered quantitative, these numbers are consistent with the values for the high residual dipolar coupling sites observed by the MQ data above.

The changes observed in the crystallization behavior of the aged DC745 materials are consistent with the changes by NMR and solvent swelling. With increasing exposure to γ-radiation, random cross-linking occurs. The result of this cross-linking is to decrease the motional mobility of the polymer chains, as seen in the NMR data, and stiffen the polymer matrix. As the cross-link density increased, the ability of the polymer chains to rearrange for crystallization decreased and the heat of fusion for melting steadily decreased, either due to slowing down of the crystallization kinetics or due to a decrease in the magnitude of the crystalline domains. The increased contribution of the filler−polymer interaction to the overall cross-link density with increased cumulative dose further reduces the ability of the polymer network to reorganize, reducing both the amount (as measured by ΔH_m) and the temperature of the crystallization.

Conclusions

We have used both Hahn-echo relaxation time measurements and ^{1}H static multiple quantum methods to assess changes in the network structure in a series of radiatively aged PDMS based elastomers based on the Dow Corning DC745 gum stock. The materials are copolymers with a complex silicon oxide filler particles and a cross-linked network. The NMR data suggest that with increasing exposure DC745 undergoes radiative cross-linking reactions that up to 250 kGy do not increase significantly the sol fraction of the network.

The MQ NMR further suggests a bimodal network with narrow distributions of residual dipolar couplings. Speciation in the two domains is dose dependent. The high residual dipolar coupling has been assigned to surface adsorbed species. The lower residual dipolar coupling spins correspond to methyl groups far from the filler surfaces.

As the polymer is exposed to increasing cumulative doses, we postulate that the following events occur: (1) an increasing number of polymer chains near the surface adsorb to the filler surface, decreasing their molecular mobility; (2) polymer chains within the network and near the interfacial chains cross-link to these interfacial chains, increasing dramatically their residual dipolar coupling; and (3) increasing cross-linking throughout the network chains as the dose increases. The increased percentage of polymer chains associated with the polymer surface would have significant impact on the time-dependent service variables that may be important for such materials, including stress relaxation and the formation of compression set.

The extension of recently reported MQ NMR methods to radiatively damaged filled systems shown in this study further demonstrates the additional insight obtainable from multiple quantum NMR analysis compared to traditional relaxation and line-shape-based methods, particularly in systems where detailed characterization of the network structure is unobtainable by other means (GPC, for example).

Acknowledgment. This work was performed under the auspices of the U.S. Department of Energy by the Lawrence Livermore National Laboratory under Contract W-7405-ENG-48. The authors thank Mark Wilson (Honeywell) for sample preparation and Jeff DeBisschop (LLNL) for sample irradiations.

References and Notes

(1) Bovey, F. A. *NMR of Polymers*; Academic: San Diego, CA, 1996.
(2) Schmidt-Rohr, K.; Spiess, H. W. *Multidimensional Solid-State NMR and Polymers*; Academic: San Diego, CA, 1994.
(3) Ando, I.; Asakura, T. *Solid State NMR of Polymers*; Elsevier Science: London, 1998.
(4) Charlesby, A.; Folland, R. *Radiat. Phys. Chem*. **1983**, *15*, 393.
(5) Folland, R.; Charlesby, A. *Radiat. Phys. Chem.* **1977**, *10*, 61.
(6) Chien, A.; Maxwell, R. S.; Chambers, D.; Balazs, B.;, LeMay, J. *J. Radiat. Phys. Chem*. **2000**, *59*, 493.
(7) Maxwell, R. S.; Balazs, B. *J. Chem. Phys.* **2002**, *116*, 10492. Note that this paper details the study of a different formulation developed by the U.S. DoE than the formulation discussed here.
(8) Maxwell, R. S.; Cohenour, R.; Sung, W.; Solyom, D.; Patel, M. *Poly. Degrad. Stab.* **2003**, *80*, 443.
(9) Cohen-Addad, J. P. *Prog. Nucl. Magn. Reson. Spectrosc.* **1993**, *25*, 1.
(10) Gronski, W.; Hoffmann, U.; Simon, G.; Wutzler, A.; Straube, E. *Rubber Chem. Technol.* **1992**, *65*, 63.
(11) Grinberg, F.; Garbarczyk, M.; Kuhn, W. *J. Chem. Phys.* **1999**, *111*, 11222.
(12) Fechete, R.; Demco, D. E.; Blumich, B. *Macromolecules* **2002,** *35*, 6083.
(13) Schneider, M. M.; Gasper, L.; Demco, D. E.; Blumich, B. *J. Chem. Phys.* **1999**, *111*, 402.
(14) Dollase, T.; Graf, R.; Heuer, A.; Spiess, H. W. *Macromolecules* **2001**, *34*, 298.
(15) Graf, R.; Heuer, A.; Spiess, H. W. *Phys. Rev. Lett.* **1998**, *80*, 5738.
(16) Graf, R.; Demco, D. E.; Hafner, S.; Spiess, H. W. *Solid State NMR* **1998**, *12*, 139.
(17) Saalwächter, K.; Ziegler, P.; Spyckerelle, O.; Haidar, H.; Vidal, A.; Sommer, J.-U. *J. Chem. Phys.* **2003**, *119*, 3468−3482.
(18) Saalwächter, K. *J. Chem. Phys.* **2004**, *120*, 454.
(19) Wang, M.; Bertmer, M.; Demco, D. E.; Blumich, B.; Litvinov, V. M.; Barthel, H. *Macromolecules* **2003**, *36*, 4411−4413.
(20) Fechete, R.; Demco, D. E.; Blumich, B. *J. Magn. Reson.* **2004**, *169*, 19.
(21) Callaghan, P. T.; Samulski, E. T. *Macromolecules* **1997**, *30*, 113.
(22) Callaghan, P. T.; Samulski, E. T. *Macromolecules.* **2000**, *33*, 3795.
(23) Grinberg, F.; Kimmich, R.; Moller, M.; Molenberg, A. *J. Chem. Phys*. **1996**, *105,* 9657.
(24) Jagadeesh, B.; Demco, D. E.; Blumich, B. *Chem. Phys. Lett.* **2004**, *393*, 416.
(25) Hafner, S.; Demco, D. E.; Kimmich, R. *Solid State NMR* **1996**, *6*, 257.
(26) Whittaker, A. K.; Bremner, T.; Zelaya, F. O. *Polymer* **1995**, *36*, 2159.
(27) Ernst, R. R.; Bodenhausen, G.; Wokaun, A. *Principles of Nuclear Magnetic Resonance in One and Two Dimensions*; Oxford University Press: New York, 1987.
(28) Kenny, J. C.; McBrierty, V. J.; Rigbi, Z.; Douglass, D. C. *Macromolecules* **1991**, *24*, 436.
(29) Luo, H.; Kluppel, M.; Schneider, H. *Macromolecules* **2004**, *37*, 8000.
(30) Saalwächter, K. *Macromolecules* **2005**, *38*, 1508.
(31) Flory, P. J. *Principles of Polymer Chemistry*; Cornell University Press: Ithaca, NY, 1953.
(32) Polmanteer, K.; Lentz, C. *Rubber Chem. Technol.* **1975**, *48*, 795.
(33) Vondracek, P.; Vallat, M. F.; Schultz, J. *J. Adhes.* **1991**, *35*, 105.
(34) French, D. *J. Appl. Polym. Sci.* **1980**, *25*, 665.
(35) Mehring, M. *Principles of High-Resolution NMR in Solids;* Springer-Verlag: Berlin, 1983.
(36) Friedrich, U.; Schnell, I.; Demco, D. E.; Spiess, H. W. *Chem. Phys. Lett.* **1998**, *285*, 49.
(37) Lorthioir, C.; Alegria, A.; Colmenero, J.; Deloche, B. *Macromolecules* **2004**, *37*, 7808.
(38) Hartmann, L.; Kremer, F.; Pouret, P.; Leger, L. *J. Chem. Phys.* **2003**, *118*, 6052.
(39) Kremer, F.; Hartmann, L.; Serghei, A.; Pouret, P.; Leger, L. *Eur. Phys. J. E* **2003**, *12*, 139.
(40) Lorthioir, C.; Auroy, P.; Deloche, B.; Gallot, Y. *Eur. Phys. J. E* **2002**, *7*, 261.
(41) Bachmann, S.; Melo, L. F. C.; Silva, R. B.; Anazawa, T. A.; Jardim, I. C. S. F.; Collins, K. E.; Collins, C. H.; Albert, K. *Chem. Mater.* **2001**, *13*, 1874.
(42) Aramata, M.; Igarashi, T. *Bunseki Kagaku* **1987**, *47*, 971.

MA047625S